



FLOW CALCULATIONS FOR A TWO-DIMENSIONAL IRRIGATION NOZZLE

Ass. Prof. Hussain Y. Mahmood
Baghdad University
College of Engineering
Mechanical Engineering
Department.

Dr. Hussain H. Ahmad
Saad General Company
Ministry of Populating
and Housing.

Munther A. Mussa
Baghdad University
College of Engineering
Mechanical Engineering
Department.

ABSTRACT

The most efficient nozzle is generally considered to be that for which the discharge coefficient is nearly unity. Nozzle dimensions influence the discharge coefficient. In sprinkler irrigation systems there are many types of nozzles because any sprinkler irrigation system has special one depend on these system characteristics, so the discharge coefficient relation with nozzle dimensions must be known to the sprinkler irrigation system designer. A computer program for nozzle flow characteristic was built and the relation between the discharge coefficient (C_d) and the nozzle geometrical dimensions to reach to the best nozzle design was studied.

The finite difference approach was introduced to carryout all computations with special grid arrangement. The steady state Navier-Stokes equations complemented with $(k - \epsilon)$ turbulence models were solved. These work calculations were for nozzle of convergent part with some angle ($3.7^\circ - 7.7^\circ$) followed by straight part (tip part). Three values were taken for the convergent part length; three for tip part length and the nozzle diameter changed for three values also. The Reynolds number range was $1.95 \times 10^5 < Re < 3.9 \times 10^5$ and Fortran 95 computer program language was used.

The results gave good imaging to the relation between nozzle dimensions and the discharge coefficient, where the major result was Increasing the tip length is allowing the boundary layer to growth and hence increasing its thickness and so discharge coefficient decreasing. Comparison of the results with ANSYS package shows that the present numerical method was accurate enough and might be used to predict the discharge coefficient for the sprinkler irrigation system nozzle.

الخلاصة

النفثات الأحسن كفاءة يعتبر عموماً الذي له معامل تدفق الأقرب إلى الواحد. معامل التدفق يتأثر بأبعاد النفثات، في منظومات الري بالررش يوجد أنواع متعددة من النفثات ذلك لان كل منظومة ري بالررش لها نفثات خاص بها يعتمد على مواصفات هذه المنظومة، لذلك علاقة معامل التدفق بأبعاد النفثات يجب أن تكون معروفة لمصمم منظومات الري بالررش. تم بناء برنامج حاسوبي لإيجاد خواص جريان النفثات وتم دراسة العلاقة بين معامل التدفق و أبعاد النفثات الهندسية للوصول إلى احسن تصميم للنفثات.

استخدمت طريقة الفروق المحددة لإنجاز الحسابات مع شبكة عقدية خاصة، معادلات Navier-Stock للحالة المستقرة بالتكامل مع نموذج $(k - \epsilon)$ للاضطراب تم حلها. الحسابات في هذا العمل تمت لنفثات ذو جزء متقارب بزواوية معين ($3.7^\circ - 7.7^\circ$) يتبعه جزء ثابت المساحة العرضية، تم اخذ ثلاثة قيم لطول الجزء

المقارب و ثلاثة لطول الجزء الثابت و ثلاثة لقطر النفاث أيضاً. مدى قيم رينولدز كان $1.95 \times 10^5 < Re < 3.9 \times 10^5$ و تم استخدام لغة الحاسبة فورتران 95. النتائج تعطي تصور جيد للعلاقة بين أبعاد النفاث و معامل التدفق حيث النتيجة الرئيسية كانت أن زيادة طول الجزء الثابت المساحة تسمح للطبقة المتاخمة أن تنمو و بالتالي زيادة سمكها وهذا يؤدي إلى نقصان معامل التدفق. مقارنة النتائج مع نتائج برنامج ANSYS أظهرت أن الطريقة المستخدمة ذات دقة كافية و ممكن استخدامها لإيجاد معامل التدفق لنفاثات منظومات الري بالرش.

KEY WORDS

Finite difference, two-dimensional, incompressible fluid, turbulent flow, sprinkler irrigation nozzle, discharge coefficient.

INTRODUCTION

The nozzle is the important part in the sprinkler irrigation system where the system dimensions, system arrangement, system ability, etc of system properties are determined by the nozzle characteristics which used, i.e. the nozzle is the main part in the system design. So the study of this part is by analyzing the flow inside it in order to have information base about this part.

In most books and researches concerned with sprinkler irrigation systems, some of nozzle characteristics are taken as constant, such as the discharge coefficient (C_d) which is usually between (85% ~ 95%) according to manufacturing goodness without taking into consideration nozzle geometrical dimensions and their effects on the flow inside the nozzle

The discharge coefficient (C_d) has a big interest especially in the sprinkler irrigation systems because its effect on the output water quantity from the system, where this quantity is a major factor in the performance determination. As an example a smaller sprinkler size in irrigation system [(FAO), 1986], found that the system requires about (300) nozzles. If these nozzles work with discharge of ($1.5 \text{ m}^3/\text{hr}$) for each nozzle, then the discharge coefficient (C_d) difference by (1%) cause on output water losses by ($4.5 \text{ m}^3/\text{hr}$). This is very big quantity had a bad effect on the system performance. This for (1%) what about for a higher values?

The first work is done in the beginning of the second half of the past century by [Miguel and Shapiro, 1956] and some of their results are still used now a days. A theory of rounded-entrance flowmeters, based on a consideration of the potential and boundary-layer flows in a convergence nozzle, is constructed and they consider only the rounded-entrance flowmeters. They found that a small change in convergent angle might produce significant alterations in discharge coefficient (C_d). [Hans, 1964] suggested an analytical expression for discharge coefficient of ASME long-radius flow nozzle with zero beta ($\beta = 0$) ratio. ASME nozzles are often used to meter the flow of water, steam and air. The flow condition in which he worked was a laminar boundary layer prevails i.e. smooth wall surface and separation was avoided (wall rounded nozzle contour). The resulting equation is: -

$$C_d = 1 - 6.528/R_N^{0.5} \quad (1)$$

[Mitsukiyo and Katayama, 1966] measured experimentally the coefficients of discharge for fire protection nozzles and discussed the results theoretically. They used various types of fire protection nozzles models of various dimensions range from ($1/2$ to $1 1/2$ in) in tip diameter. They found that the values of discharge coefficients have a close relationship with character of boundary layer.

Shortening of nozzle tip will result directly in less friction loss in a nozzle only when the nozzle boundary is covered with a wholly laminar or turbulent boundary layer.

[Benedict and Wyler, 1978] developed theoretically a new nozzle discharge coefficient for ASME elliptical nozzles. This discharge coefficient based on an axisymmetric boundary layer solution, which in turn is based on a new axisymmetric potential flow solution., a new formulation of the discharge coefficient results for ASME flow nozzle as follow: -

$$C_d = \left(1 - 4 \frac{\delta^*}{D_2}\right) \left[\frac{1 - 4\delta^*/D_2}{1 - 4\delta^*/D_2 - 4\delta^{**}/D_2} \right]^{1/2} \quad (2)$$

So they concluded from this equation that the discharge coefficient for ASME nozzles will be influenced by the energy thickness (δ^{**}) as well as by the displacement thickness (δ^*).

[Jackson and Davis, 2001] studied jet production for hydraulic mining of china clay. The prime objective of their work is to maximize jet momentum flux at an excavation face. They based their study on the fact that delayed jet break-up produces an increase in jet impact momentum flux and that careful nozzle design leads to more coherent jets. So they suggested a systematic method for nozzle design which should lead to maximum possible jet impact momentum fluxes. They obtained that a reduction in nozzle wall length leads to a significant reduction in exit values of displacement thickness (δ^*) and according to the equation (2)[(FAO), 1986] the reduction in nozzle wall length leads to a significant maximize in the discharge coefficient (C_d) i.e. in nozzle performance.

$$C_d = 1 - 4 \frac{\delta^*}{D_2} \quad (3)$$

The present work aimed to study the sprinkler irrigation nozzles flow characteristic by using theoretical techniques, which depends on some fundamental equations deemed by previous researchers to build a computer program for nozzle flow characteristic. The program may be applied to any similar nozzle when due allowance is made for the constraints of that nozzle also find the relation between the discharge coefficient (C_d) and the nozzle geometrical dimensions to reach to the best nozzle design, which has discharge coefficient (C_d) nearest to unity.

The present search gives a theoretical study for the flow characteristics inside two-dimensional nozzle of incompressible fluid (water). The nozzle consists of convergent part with some angle followed by straight part (tip part). The convergent part length, the straight part length and the nozzle diameter will be changed for different values to investigate the effect of the nozzle geometrical dimensions on the flow characteristics inside it.

A mathematical model will be specified consist of conservation of mass and conservation of momentum equations, which describe the incompressible turbulent flow inside this nozzle by using ($k - \epsilon$) turbulence model and A computational solution of these equations will be by using finite - difference method (FDM).

NOZZLE GEOMETRY

The geometry of the nozzle under consideration is a common model, used in sprinkler irrigation systems with different dimensions. It consists of convergent part with some angle followed by a straight part (tip part) **Fig. (1)**.

In most sprinkler irrigation systems the nozzle dimensions ranges within the following values [(FAO), 1986]: -

$$D_1 = 10 \sim 20 \text{ mm}$$

$$D_2 = 5 \sim 10 \text{ mm}$$

$$L_1 = 18.5 \sim 77 \text{ mm}$$

$$L_2 = 4 \sim 12 \text{ mm}$$

The problem is 2D incompressible turbulent flow. In analysis Cartesian Co-Ordinate system is used to avoid the complexity of the polar Co-Ordinate system and the small dimensions of the model permits to take this simplification [Aness AL-Fakhri, 1981].

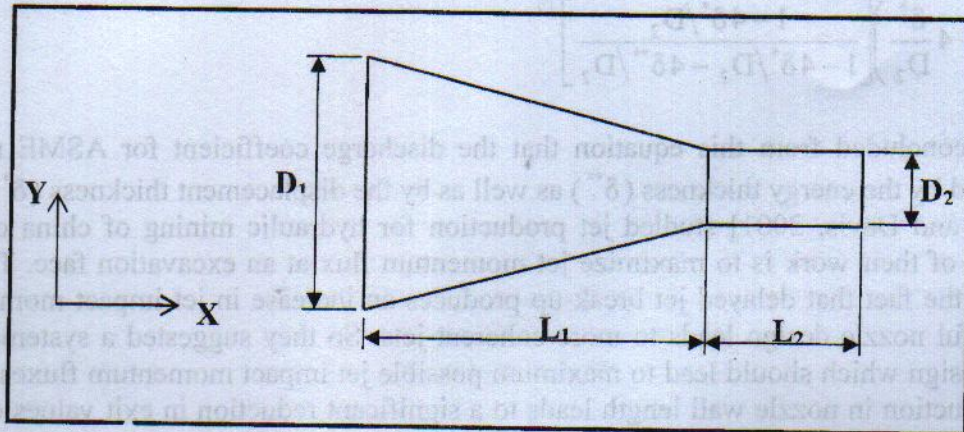


Fig. (1) Nozzle geometry

BASIC EQUATIONS

Using time averaged of the instantaneous conditions, the time averaged steady state conservation equations for mass, momentum, and transport equations of turbulence can be written in a general tensor form as follows [Habib and McEligot, 1982]: -

Continuity Equation

$$\frac{\partial u_j}{\partial x_j} = 0 \quad (4)$$

Momentum Equation

$$\frac{\partial}{\partial x_j} \left(\rho u_i u_j + \rho \overline{u_i u_j} \right) = - \frac{\partial p}{\partial x_i} \quad (5)$$

Transport Equation of Turbulence

The standard form of \$k - \epsilon\$ model is as follow [Launder and Spalding, 1974]: -

Turbulence kinetic energy equation

$$\frac{\partial}{\partial x_j} (\rho u_j k) = \frac{\partial}{\partial x_j} \left(\frac{\mu_{eff}}{\sigma_k} \frac{\partial k}{\partial x_j} \right) + G - \rho \epsilon \quad (6)$$

And dissipation of turbulence kinetic energy equation



$$\frac{\partial}{\partial x_j} (\rho u_j \epsilon) = \frac{\partial}{\partial x_j} \left(\frac{\mu_{eff}}{\sigma_\epsilon} \frac{\partial \epsilon}{\partial x_j} \right) + c_{\epsilon 1} \frac{\epsilon}{k} G - c_{\epsilon 2} \rho \frac{\epsilon^2}{k} \quad (7)$$

Where $G = \mu_t \left(\frac{\partial u_i}{\partial x_j} + \frac{\partial u_j}{\partial x_i} \right) \frac{\partial u_i}{\partial x_k} - \frac{2}{3} \frac{\partial u_j}{\partial x_j} \left(\mu_t \frac{\partial u_\lambda}{\partial x_\lambda} + \rho k \right)$

The turbulent viscosity μ_t is related to the turbulent kinetic energy (k) and to the dissipation of turbulent kinetic energy (ϵ) through the expression [Jones and Launder, 1972]: -

$$\mu_t = c_\mu \rho \frac{k^2}{\epsilon} \quad (8)$$

And the effective viscosity (μ_{eff}) is related to the turbulent viscosity (μ_t) and to the laminar viscosity (μ_l) (its material property) through the relation: -

$$\mu_{eff} = \mu_l + \mu_t \quad (9)$$

In the above equations ($c_\mu, c_{\epsilon 1}, c_{\epsilon 2}, \sigma_k, \sigma_\epsilon$) are constants at high Reynolds number values and their values are shown in **Table (1)** [Launder and Spalding, 1974]: -

Table (1) Constants of turbulent transport equations

c_μ	$c_{\epsilon 1}$	$c_{\epsilon 2}$	σ_k	σ_ϵ
0.09	1.44	1.92	1.0	1.3

To solve these equations some assumptions should be taken to fit the case, which is under study.

These assumptions are: -

- 1-steady state flow.
- 2-two dimensional flow.
- 3-incompressible and isothermal flow.
- 4-turbulent flow.
- 5-no inlet swirl.

GOVERNING EQUATIONS

According to the assumptions maintained above the basic equation is reduced to the following: -

Continuity Equation

$$\frac{\partial u}{\partial x} + \frac{\partial v}{\partial y} = 0 \quad (10)$$

Momentum Equation

$$\rho u \frac{\partial u}{\partial x} + \rho v \frac{\partial u}{\partial y} = - \frac{\partial p}{\partial x} + \frac{\partial}{\partial x} \left(\mu_{eff} \frac{\partial u}{\partial x} \right) + \frac{\partial}{\partial y} \left(\mu_{eff} \frac{\partial u}{\partial y} \right) + \frac{\partial}{\partial x} \left(\mu_t \frac{\partial u}{\partial x} \right) + \frac{\partial}{\partial y} \left(\mu_t \frac{\partial v}{\partial x} \right) - \frac{2}{3} \rho \frac{\partial k}{\partial x} \quad (11)$$

Turbulence Kinetic Energy Equation

$$\rho u \frac{\partial k}{\partial x} + \rho v \frac{\partial k}{\partial y} = \frac{\partial}{\partial x} \left(\frac{\mu_{eff}}{\sigma_k} \frac{\partial k}{\partial x} \right) + \frac{\partial}{\partial y} \left(\frac{\mu_{eff}}{\sigma_k} \frac{\partial k}{\partial y} \right) + G - \rho \epsilon \tag{12}$$

Dissipation Turbulence Kinetic Energy Equation

$$\rho u \frac{\partial \epsilon}{\partial x} + \rho v \frac{\partial \epsilon}{\partial y} = \frac{\partial}{\partial x} \left(\frac{\mu_{eff}}{\sigma_k} \frac{\partial \epsilon}{\partial x} \right) + \frac{\partial}{\partial y} \left(\frac{\mu_{eff}}{\sigma_k} \frac{\partial \epsilon}{\partial y} \right) + c_{\epsilon 1} \frac{\epsilon}{k} G - c_{\epsilon 2} \rho \frac{\epsilon^2}{k} \tag{13}$$

Where $G = \mu_t \left[2 \left(\frac{\partial u}{\partial x} \right)^2 + 2 \left(\frac{\partial v}{\partial y} \right)^2 + \left(\frac{\partial u}{\partial y} + \frac{\partial v}{\partial x} \right)^2 \right]$

These equations and the eq. (8) and (9) mentioned previously describe the problem mathematically.

DISPLACEMENT THICKNESS (δ^*)

The displacement thickness measures the amount by which a streamline is displaced due to boundary layer existence. It is computed from the following equation: -

$$\delta^* = 2 \int_0^{D_2/2} \left(1 - \frac{u}{u_c} \right) dy \tag{14}$$

COEFFICIENT OF DISCHARGE (C_d)

The main goal of our work is to obtain the discharge coefficient (C_d) which is related to nozzle efficiency, generally the efficiency of the nozzle would be maximum if the discharge coefficient (C_d) reaches unity. Many attempts have been made in the past to predict discharge coefficient, in spite of large rigorous formulation of (C_d) in terms of exit boundary layer parameters for nozzles and venturimeters. The approximation to the original equation of [Miguel and Shapiro, 1956] used by [Hall, 1959] is sufficiently accurate and largely used for many engineering purposes: -

$$C_d = \left(1 - 4 \frac{\delta^*}{D_2} \right) \tag{15}$$

BOUNDARY CONDITIONS

In the case under study, boundary conditions in four sides must be satisfied to describe the problem of Fig. (1), one in inlet section, two for the two sides (walls) and the last one at the exit section.

$$p_{in} = 300000 \sim 350000 \text{ pa } \text{ [(FAO),1986]} \tag{16}$$

$$u_{in} = \sqrt{\frac{2p_{in}}{3\rho}} \tag{17}$$

The turbulence kinetic energy and dissipation kinetic energy is from the following equation [Morsi and Clayton, 1986]: -

$$k_{in} = c_k u_{in}^2 \tag{18}$$



$$\varepsilon_{in} = \frac{1.5(c_\mu k_{in})}{0.5(c_\varepsilon D_1)} \quad (19)$$

$$p_e = 0 \quad (20)$$

$$u_{wall} = 0 \quad (21)$$

$$v_{wall} = 0 \quad (22)$$

$$\left. \begin{aligned} k_{wall} &= 0 \\ \frac{\partial \varepsilon}{\partial y} \Big|_{wall} &= 0 \end{aligned} \right\} \quad (23)$$

Where: - $c_k = 0.003$, $c_\varepsilon = 0.03$

WALL FUNCTION

Inside the zone close to the wall, the flow is controlled by molecular viscosity and changes are steepest [Hinze, 1975]. Therefore, there is a requirement on the grid scheme to provide many more points close to the wall than in the central zone of the nozzle. This lead to the use of unequal grid spacing. If equal grid spacing is employed for turbulent flow situation, then a large number of grid points will be required. This may introduce accumulation of errors and cause large computer time usage.

An economical method is to introduce the wall function [Lauder and Spalding, 1974], which is a special formula for evaluating the effective exchange coefficient at the wall (Γ_{wall}). This method is the one that has been widely used and is still preferred for many practical purposes. Its merits are two: it economize computer time and storage also it allows the introduction of additional empirical information in special cases when the wall is rough. For the evaluation of turbulent kinetic energy and dissipation turbulent kinetic energy, it is suffice to fix their values at the near wall node according to the following formula [Wang and Komori, 1998]: -

$$k_{wall} = \frac{\tau_{wall}}{\rho C_\mu^{1/2}} \quad (24)$$

$$\varepsilon_{wall} = \frac{C_\mu^{3/4} k^{3/2}}{v_k \Delta y} \quad (25)$$

Table (2) summarizes the expression of effective exchange coefficient at the wall (Γ_{wall}) for different dependant variables [Patanker, 1980].

Table (2) Wall function

Φ	Γ_{wall}
Velocity component normal to the wall (v)	0
Velocity component parallel to the wall (u)	$y^+ > 11.5 \quad \mu = \frac{\mu_1 y^+ v_k}{\ln(E.y^+)}$ $y^+ \leq 11.5 \quad \mu = \mu_1$
k_{wall}	Not required
ε_{wall}	Not required

$$y^+ = \frac{\rho C_{\mu}^{1/4} k^{1/2} \Delta y}{\mu_1} \quad (26)$$

Where (Δy) is the normal distance of the near wall node to the solid surface. In the above formula (v_k) is the Von Karman constant (0.4187) and (E) is an integration constant that depend on the roughness of the wall. For a smooth wall with constant shear stress, (E) has a value of (9.793) [Patanker, 1980].

GRID GENERATION

In case of vary cross sectional area flow present the additional complication to finite difference analysis that the total number of transverse mesh point (nodes) and/or the transverse mesh size will not remain constant as each axial step is taken. To solve this problem [Hornbeck, 1975] presented a method by which adjust the axial step size (Δx) so that exactly one transverse grid point is subtracted (or added) while maintaining the same transverse grid size (Δy) Fig. (2). In this method every node has neighboring nodes in the axis, two in x-direction and two in y-direction.

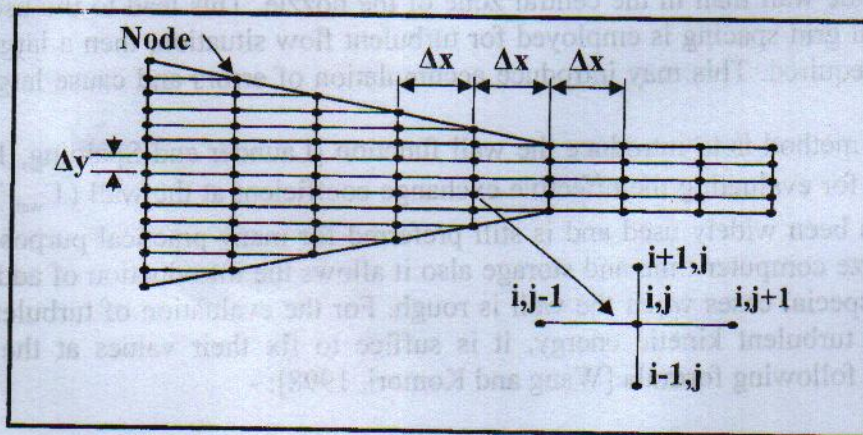


Fig. (2) Used mesh generation technique.

THE DISCRETISATION EQUATION

If the governing equations are taken and every term is replaced by its equivalent algebraic terms by F.D.M technique and rearrange, the following discretisation equations will be obtained: -

Momentum Equation

$$u_{i,j}^{T+1} = (1-\omega)u_{i,j}^T + \frac{\omega}{ax_1} \left[ax_2 u_{i+1,j}^T + ax_3 u_{i-1,j}^T + ax_4 u_{i,j+1}^T + ax_5 u_{i,j-1}^T - \frac{1}{\Delta x} (p_j - p_{j-1}) + SX \right] \quad (27)$$

Where: -



$$ax_1 = \left[\frac{\rho u_{i,j}}{\Delta x} + \frac{\rho v_{i,j}}{\Delta y} + \frac{\mu_{eff_{i,j+1}} + \mu_{eff_{i,j}}}{2\Delta x^2} + \frac{\mu_{eff_{i,j}} + \mu_{eff_{i,j-1}}}{2\Delta x^2} + \frac{\mu_{eff_{i+1,j}} + \mu_{eff_{i,j}}}{2\Delta y^2} + \frac{\mu_{eff_{i,j}} + \mu_{eff_{i-1,j}}}{2\Delta y^2} + \frac{\mu_{t_{i,j+1}} + \mu_{t_{i,j}}}{2\Delta x^2} + \frac{\mu_{t_{i,j}} + \mu_{t_{i,j-1}}}{2\Delta x^2} \right]$$

$$ax_2 = \left[\frac{\mu_{eff_{i+1,j}} + \mu_{eff_{i,j}}}{2\Delta\Delta^2} \right], ax_3 = \left[\frac{\rho v_{i,j}}{\Delta y} + \frac{\mu_{eff_{i,j}} + \mu_{eff_{i-1,j}}}{2\Delta\Delta^2} \right], ax_4 = \left[\frac{\mu_{eff_{i,j+1}} + \mu_{eff_{i,j}} + \mu_{t_{i,j+1}} + \mu_{t_{i,j}}}{2\Delta\Delta^2} \right],$$

$$ax_5 = \left[\frac{\rho u_{i,j}}{\Delta x} + \frac{\mu_{eff_{i,j}} + \mu_{eff_{i,j-1}} + \mu_{t_{i,j}} + \mu_{t_{i,j-1}}}{2\Delta\Delta^2} \right]$$

The pressure term appears in momentum equation is treated by use the following equation: -

$$(p_j - p_{j-1}) = \frac{\dot{m} - \int \rho \alpha_{i,j} dy}{\int \rho \beta_{i,j} dy} \tag{28}$$

Where: -

$$\alpha_{i,j} = \frac{1}{ax_1} [ax_2 u_{i+1,j} + ax_3 u_{i-1,j} + ax_4 u_{i,j+1} + ax_5 u_{i,j-1} + SX] \& \beta_{i,j} = -\frac{1}{ax_1 \Delta x}$$

Continuity Equation

$$v_{i,j} = (1 - \omega)v_{i,j} + \omega \left[v_{i-1,j} + \frac{\Delta y}{\Delta x} (u_{i,j-1} - u_{i,j}) \right] \tag{29}$$

Turbulence kinetic Energy

$$ak_1 k_{i,j} = ak_2 k_{i+1,j} + ak_3 k_{i-1,j} + ak_4 k_{i,j+1} + ak_5 k_{i,j-1} + G - \rho \epsilon_{i,j} \tag{30}$$

Where: -

$$ak_1 = \left[\frac{\rho u_{i,j}}{\Delta x} + \frac{\rho v_{i,j}}{\Delta y} + \frac{\mu_{eff_{i,j+1}} + \mu_{eff_{i,j}}}{2\sigma_k \Delta x^2} + \frac{\mu_{eff_{i,j}} + \mu_{eff_{i,j-1}}}{2\sigma_k \Delta x^2} + \frac{\mu_{eff_{i+1,j}} + \mu_{eff_{i,j}}}{2\sigma_k \Delta y^2} + \frac{\mu_{eff_{i,j}} + \mu_{eff_{i-1,j}}}{2\sigma_k \Delta y^2} \right]$$

$$ak_2 = \left[\frac{\mu_{eff_{i+1,j}} + \mu_{eff_{i,j}}}{2\sigma_k \Delta y^2} \right], ak_3 = \left[\frac{\rho v_{i,j}}{\Delta y} + \frac{\mu_{eff_{i,j}} + \mu_{eff_{i-1,j}}}{2\sigma_k \Delta y^2} \right],$$

$$ak_4 = \left[\frac{\mu_{eff_{i,j+1}} + \mu_{eff_{i,j}}}{2\sigma_k \Delta x^2} \right], ak_5 = \left[\frac{\rho u_{i,j}}{\Delta x} + \frac{\mu_{eff_{i,j}} + \mu_{eff_{i,j-1}}}{2\sigma_k \Delta x^2} \right]$$

Dissipation Turbulence Kinetic Energy

$$a\epsilon_1 \epsilon_{i,j} = a\epsilon_2 \epsilon_{i+1,j} + a\epsilon_3 \epsilon_{i-1,j} + a\epsilon_4 \epsilon_{i,j+1} + a\epsilon_5 \epsilon_{i,j-1} + C_{\epsilon_1} \frac{\epsilon_{i,j}}{k_{i,j}} G \quad (31)$$

Where: -

$$a\epsilon_1 = \left[\frac{\rho u_{i,j}^*}{\Delta x} + \frac{\rho v_{i,j}}{\Delta y} + \frac{\mu_{\text{eff},i,j+1} + \mu_{\text{eff},i,j}}{2\sigma_\epsilon \Delta x^2} + \frac{\mu_{\text{eff},i,j} + \mu_{\text{eff},i,j-1}}{2\sigma_\epsilon \Delta x^2} + \frac{\mu_{\text{eff},i+1,j} + \mu_{\text{eff},i,j}}{2\sigma_\epsilon \Delta y^2} + \frac{\mu_{\text{eff},i,j} + \mu_{\text{eff},i-1,j}}{2\sigma_\epsilon \Delta y^2} + C_{\epsilon_2} \rho \frac{\epsilon_{i,j}}{k_{i,j}} \right]$$

$$a\epsilon_2 = \left[\frac{\mu_{\text{eff},i+1,j} + \mu_{\text{eff},i,j}}{2\sigma_\epsilon \Delta y^2} \right], a\epsilon_3 = \left[\frac{\rho v_{i,j}}{\Delta y} + \frac{\mu_{\text{eff},i,j} + \mu_{\text{eff},i-1,j}}{2\sigma_\epsilon \Delta y^2} \right],$$

$$a\epsilon_4 = \left[\frac{\mu_{\text{eff},i,j+1} + \mu_{\text{eff},i,j}}{2\sigma_\epsilon \Delta x^2} \right], a\epsilon_5 = \left[\frac{\rho u_{i,j}}{\Delta x} + \frac{\mu_{\text{eff},i,j} + \mu_{\text{eff},i,j-1}}{2\sigma_\epsilon \Delta x^2} \right]$$

NUMERICAL ALGORITHM

The solution manner is depending on the repeated iterative to reach the final results. This repeated iterative consists of two parts; the major is the iteration over the complete solution procedure to obtain the unknowns final values. The second consists of a group of inner iteration to reach the value of this unknown in every loop of the major iteration. The iteration sequence is repeated until the residual errors fall below a certain value representing the converged solution. The total maximum residual error is taken to be 1×10^{-4} [Patanker, 1980].

RESULTS AND DISCUSSION

These results for a nozzle consists of convergent part with some angle followed by straight part (tip part). Three values are taken for the convergent part length (L_1), three for the tip part length (L_2) and the nozzle diameter (D_1) changed for three values also.

As shown in this **Fig. (3)** the results were obtained in five sections of the flow. The first section at the point ($L=1/3 L_1$), the second section at the point ($L=2/3 L_1$), the third section at contraction point ($L=L_1$), the fourth section at half-length of the constant area part ($L=L_1 + 1/2 L_2$), and the fifth section at the nozzle exit ($L=L_1 + L_2$).

The pressure values drops from the maximum value at the nozzle inlet (350000 pa) to the minimum value (atmosphere pressure) at the nozzle exit. And since the total length of the nozzles was short then the dropping would be sharp, this sharpness was increased with increasing the convergence angle values as noted from **Fig. (3)** and thus the turbulence is increased.

Referring to **Fig. (4)** noticed that the tip length increasing lead to decreasing on the discharge coefficient values for all study cases, this decreasing was clear especially in the case of small diameter of the nozzles. This decrease is caused by the addition length allow the boundary layer growth and its thickness increased. From comparison between **Fig. (4 & 5)** noticed that the discharge coefficient values increased by increasing the convergence angle values for all the cases, this because the turbulence increasing and so boundary layer thickness is decreasing

From **Fig. (6)** it is noticed that the boundary layer thickness in the first section is larger than that in the other sections. In the last three sections the boundary layer thickness is equal, but the difference is in the region of contact between the boundary layer and the core flow. In the first section the angle of contact was obtuse angle. In the second section the sharpness of the angle was began. In the third section this angle was clearly became acute angle. In the fourth section it return to diverge

and in the fifth section this diverge was not increased. Using ANSYS package checked these results. A good agreement was found in the case where ($D_1=10$ mm, $L_1=18.5$ mm) with the present work Fig. (7).

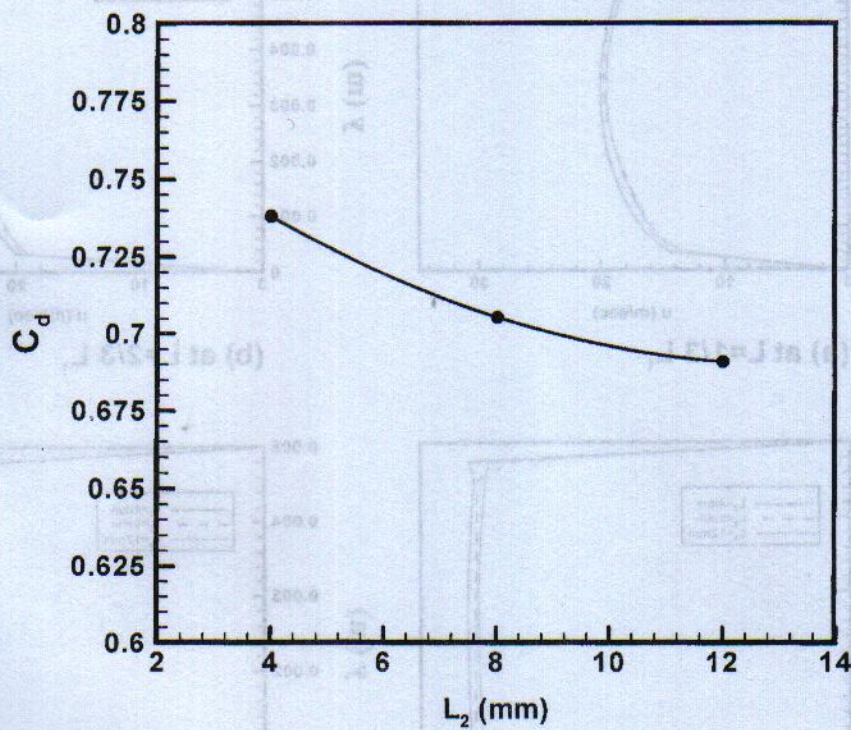


Fig. (4) Tip length effect on the discharge coefficient for $D_1=10$ mm, $L_1=18.5$ mm.

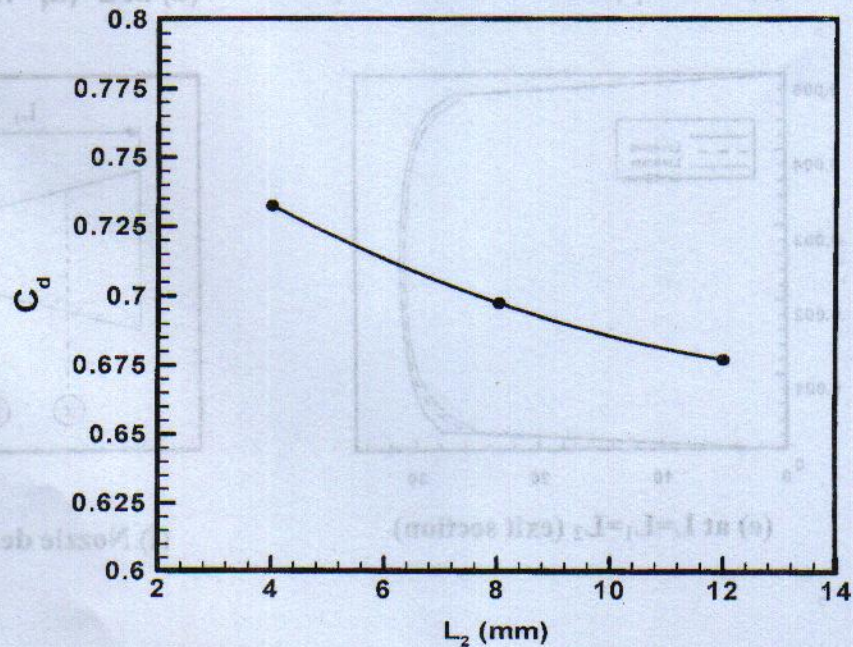
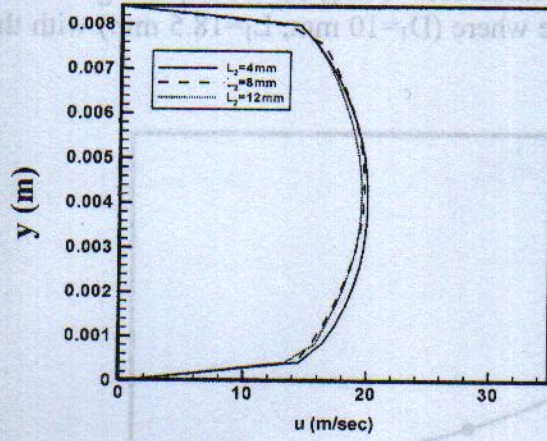
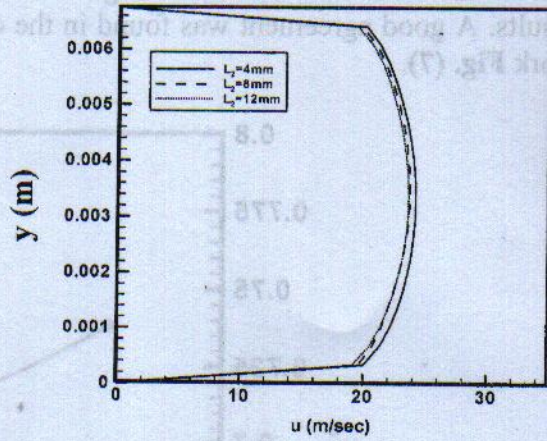


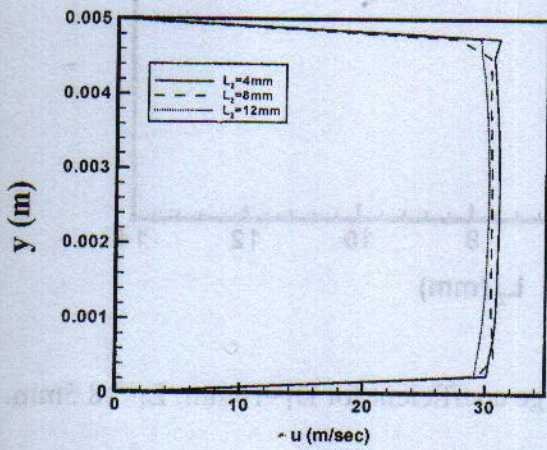
Fig. (5) Tip length effect on the discharge coefficient for $D_1=10$ mm, $L_1=28.5$ mm.



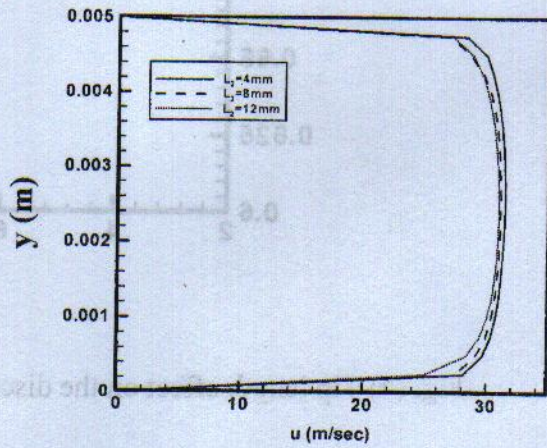
(a) at $L=1/3 L_1$



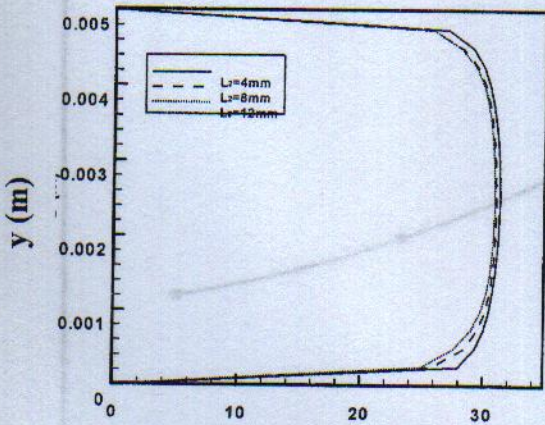
(b) at $L=2/3 L_1$



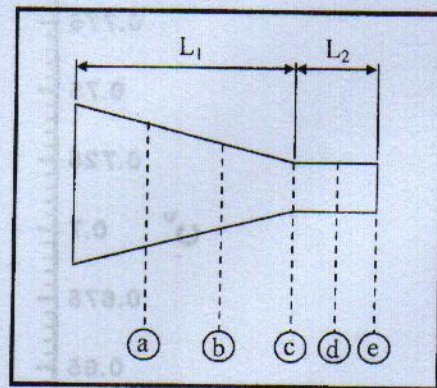
(c) at $L=L_1$ (contraction section)



(d) at $L=(L_1+1/2 L_2)$



(e) at $L=L_1=L_2$ (exit section)



(f) Nozzle description

Fig. (6) Axial velocity profile for $D_1=10\text{mm}$, $L_1=18.5\text{mm}$.

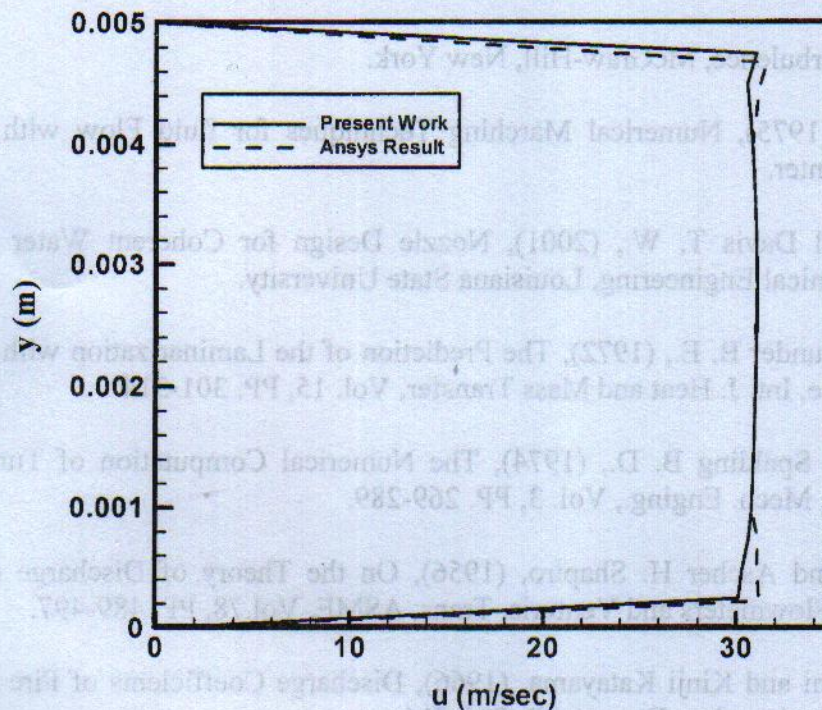


Fig. (7) Comparison of present work with ANSYS package results, at contraction section for $D_1=10\text{mm}$, $L_1=18.5\text{mm}$.

CONCLUSIONS

From the present work results, for the nozzle that's described previously, the following conclusions can be obtained: -

- 1- Increasing the convergence angle will increase the turbulence due to the increase of the sharpness of the angle between boundary layer and core flow region.
- 2- Increasing the tip length allowing the boundary layer to grow and hence increasing its thickness.
- 3- Turbulence increase leads to boundary layer thickness decrease and so the discharge coefficient is increasing.

REFERENCES

- Aness AL-Fakhri, (1981), Prediction and Measurement of Turbulent Flow and Heat Transfer in Annular Channel of Constant and Varying Cross Section Area, Ph.D.Thesis, Mech.Eng.Dept., University of Manchester.
- Benedict R. P. and Wyler J. S., (1978), Analytical and Experimental Studies of ASME Flow Nozzles, Trans. ASME. J. of Fluids Engineering, Vol.100, PP. 256-275.
- Habib M. A. and McEligot D. M., (1982), Turbulent Heat Transfer in A Swirl Flow Downstream of An Abrupt Pipe Expansion, International Heat Transfer Conference, Vol.3, PP. 159-164.
- Hall G.W., (1959), Application of Boundary Layer Theory to Explain Some Nozzle and Venturimeter Flow Peculiarities, Proc. Inst. Mech. Engs., Vol. 173, No. 36, PP. 837-870.

Hans J. Leuthesser, (1964), Flow Nozzles With Zero Beta Ratio, ASME J. of Basic Engineering, Sept. PP. 538-542.

Hinze J., (1975), Turbulence, McGraw-Hill, New York.

Hornbeck R. W., (1975), Numerical Marching Techniques for fluid Flow with Heat Transfer, NASA Research Center.

Jackson M. K. and Davis T. W., (2001), Nozzle Design for Coherent Water Jet Production, Department of Chemical Engineering, Louisiana State University.

Jones W. P. and Launder B. E., (1972), The Prediction of the Laminarization with a two-Equation Model of Turbulence, Int. J. Heat and Mass Transfer, Vol. 15, PP. 301-314.

Launder B. E. and Spalding B. D., (1974), The Numerical Computation of Turbulent Flow, J. Compt. Meth. Appl. Mech. Enging., Vol. 3, PP. 269-289.

Miguel A. Rivas and Ascher H. Shapiro, (1956), On the Theory of Discharge Coefficients for Rounded-Entrance Flowmeters and Venturis, Trans. ASME, Vol.78, PP. 489-497.

Mitsukiyo Murakami and Kinji Katayama, (1966), Discharge Coefficients of Fire Nozzles, Trans. ASME J. of Basic Engineering, Decem. PP. 706-716.

Morsi Y. S. and Clayton B. R., (1986), Determination of Principal Characteristics of Turbulent Swirling Flow Along Annuli, Int. J. Heat and Fluid Flow, Vol. 7, PP. 208-222.

Patanker S. V., (1980), Numerical Heat Transfer and Fluid Flow, McGraw-Hill, New York.

The international Food and Agriculture Organization (FAO), (1986), Sprinkler Irrigation Systems, London.

Wang Y. and Komori S., (1998), Simulation of the Subsonic Flow in A High-Speed Centrifugal Compressor Impeller by the Pressure-Based Method, Proc. Inst. Mech. Engs., Part A, Vol.212, PP. 269-287.

NOMENCLATURE

Symbol	Description	Unit
$C_{\mu}, C_{\epsilon 1}, C_{\epsilon 2}$	Constant in the $k - \epsilon$ model	
E	Constant used in the law of the wall	
G	Generation term	kg/m.s ³
k	Turbulence kinetic energy	m ² /s ²
m	Nodes number in x-direction	
\dot{m}	Mass flow rate	kg/s
n	Nodes number in y-direction	
p	Pressure	N/m ²
u	Axial velocity	m/s
v	Radial velocity	m/s
x	Cartesian axial co-ordinate	
y	Cartesian radial co-ordinate	



y_p Normal distance from wall surface to the adjacent node m

Greek Symbols

ω	Relaxation factor	
Γ_{wall}	Diffusion coefficient at the wall	kg/m.s
ε	Dissipation rate of turbulent kinetic energy	m^2/s^3
κ	Von Karman constant	
μ_l	Laminar viscosity	kg/m.s
μ_t	Turbulent viscosity	kg/m.s
μ_{eff}	Effective eddy viscosity	kg/m.s
ρ	Fluid density	kg/m^3
$\sigma_k, \sigma_\varepsilon$	Constant in the k - ε model	

Superscripts

'	Averaged quantity
'	Fluctuated quantity
T	Iteration number

Subscripts

(i,j)	Grid nodes in (x,y) direction
p	Adjacent wall node
wall	Wall node
l	Laminar
t	Turbulence
k	Turbulence kinetic energy equation
ε	Dissipation Turbulence kinetic energy equation
in	Inlet
out	Outlet

Abbreviations

FDM	Finite difference method
SUR	Successive under-relaxation